Detection of Diamonds in Kimberlite by the Tagged Neutrons Method

Aleksakhin V. Yu., Bystritsky V. M., Zamyatin N. I., Zubarev E. V., Krasnoperov A. V., Rapatsky V. L., Rogov Yu. N., Sadovsky A. B., Salamatin A. V., Salmin R. A., Sapozhnikov M. G., Slepnev V. M., Khabarov S. V.

Neutron Technologies LLC, Dubna
Joint Institute for Nuclear Research, Dubna

Razinkov E. A., Tarasov O. G.

Neutron Technologies LLC, Dubna

Nikitin G. M.

Institute "Yakutniproalmaz", ALROSA JSC, Mirny

Abstract

A new technology for diamond detection in kimberlite based on the tagged neutron method is proposed. The results of experimental researches on irradiation of kimberlite samples with 14.1-MeV tagged neutrons are discussed. The source of the tagged neutron flux is a portable neutron generator with a built-in 64-pixel silicon alpha detector with double-sided stripped readout. Characteristic gamma rays resulting from inelastic neutron scattering on nuclei of elements included in the composition of kimberlite are registered by six gamma ray detectors based on BGO crystals. The criterion for diamond presence in kimberlite is an increased carbon concentration within a certain volume of kimberlite sample.

1. Introduction

At present the kimberlite ore is processed in crushers or grinding rolls with subsequent grinding in wet mills down to a size of 0.2 mm and less. Ore is concentrated by X-ray fluorescent, gravitation, and flotation methods [1]. X-ray fluorescence separation uses diamond property to luminesce under X-ray exposure. An X-ray fluorescence separator automatically cuts out the bulk of the ore concentrate that contains detected diamonds.

The basic disadvantage of the standard diamond processing technology is that crushing kimberlite ore can break the most valuable large diamonds of few carats or larger.

We would like to propose a new procedure for non-destructive detection of large-sized diamonds in kimberlite. The main idea is irradiation of large kimberlite pieces with fast neutrons with an energy of 14 MeV produced in the binary nuclear reaction

$$d + {}^3H \rightarrow {}^4He + n. \quad (1)$$

Direction of a neutron is determined by detecting (tagging) of the α-particle that accompanies the neutron using a special α-detector. Interacting with kimberlite, tagged neutrons induce inelastic scattering reactions

$$n + A \rightarrow n + A^* \rightarrow n + \gamma + A. \quad (2)$$

During de-excitation of nuclei A^* γ-quanta are emitted with an energy spectrum specific for each chemical element included in the kimberlite . Characteristic γ-rays are registered by gamma detectors in coincidence with the signal from the α-detector. Measurement of the time interval between the signals from the α- and γ-detectors allows determining the distance from the neutron source to the point from which the γ-quantum is emitted since the neutron speed is constant and equals 5 cm/ns. Thus the tagged neutron method makes it possible to determine all three spatial coordinates of the examined sample volume.

Lately the tagged neutron method (also called Associated Particle Imaging (API) method) has been widely used [2-12] for creating explosives and drug detectors, which allow determining elemental composition of the substance hidden in the examined objects of various sizes from hand luggage to shipping containers.

The search for diamonds by the tagged neutron method is reduced to detection of excess carbon at a particular point of the kimberlite sample. Large penetrability of fast neutrons makes it possible to examine appreciably large samples of kimberlite. The ability of the tagged neutron method to determine the three-dimensional position of the explored object allows not only revealing the presence of a large-size diamond in a rock piece but also locating its position in the sample. Thus, rock pieces containing large-size diamonds can be identified before the crushing stage.

We developed a method for automatic detection of diamonds in kimberlite and created an experimental diamond detection setup, which we used to carry out experiments on estimation of detectable diamond size for various background conditions.

2. Description of the setup

The experimental setup for diamond detection in kimberlite consists of a portable neutron generator ING-27 with a built-in 64-pixel alpha detector, six gamma detectors based on BGO crystals, electronics of the data acquisition system for the alpha and gamma detectors, and power supply units for the neutron generator and the alpha and gamma detectors. The general view of the setup is given in Fig. 1.

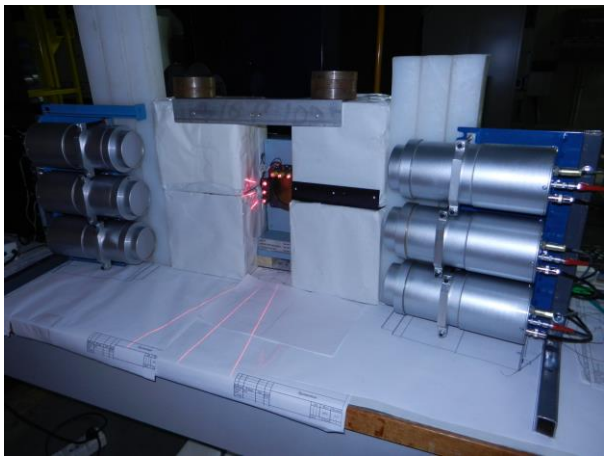

Fig. 1. General view of the experimental setup.

In the foreground of Fig. 1 there are 6 gamma detectors with their BGO crystals protected with steel shielding against direct neutrons emitted by ING-27. The area of the tagged neutron beams irradiating the investigated object is outlined with 6 laser line generators fixed on the neutron generator housing. The diamond simulant is attached to a set of suspension wires, which can also hold several kimberlite samples. The diamond simulant is typically located behind the kimberlite sample, as shown in Fig. 2.

Fig. 2. Diamond simulant weighing1.78 g behind a kimberlite sample.

In some cases the diamond simulant is placed between two samples of natural kimberlite.

2.1 Neutron generator

The ING-27 neutron generator is developed by the All-Russian Research Institute of Automatics, Moscow, and has the following characteristics:

Maximum intensity	$7 \cdot 10^7$ s^{-1}
Neutron energy	14.1 MeV
Mode of neutron radiation	constant
Power supply	200±5 V
Maximum consumed power	40 W
Size	130 x 279 x 227 mm
Weight	8 kg
Service life	800 h

Inside the neutron generator there is a 64-pixel silicon alpha detector developed at the Joint Institute for Nuclear Research (Dubna). The alpha detector provides 64 beams of tagged neutrons.

2.2 Alpha detector

The silicon α-detector built into the neutron generator is a double-sided stripped detector, which consists of 8 mutually perpendicular strips on each side forming an 8 x 8 matrix of 4 x 4 mm^2 elements. The total sensitive area of the 64-element α-detector is 32 x 32 mm^2. The alpha detector is located 62 mm away from the tritium target of the ING-27. The front-end electronics unit of the alpha detector consists of 16 independent single amplifiers fed from 16 strips of the alpha detector. Signal preamplifiers of the alpha detector are mounted in the rear part of the neutron generator.

In order to detect diamonds it is important to know precisely the spatial distribution of the tagged neutron beams, as the objects to be detected are about 10–20 mm in size. Spatial characteristics of 64 tagged neutron beams were measured by a scintillation stripped detector. It turns out that the widths of the tagged neutron beams and the positions of the peak centres agrees to the values expected for the point-like deuteron beam on the target.

At a distance of 20 cm from the neutron generator target the size of each tagged beam in the plane perpendicular to the direction of the tagged beam is 13 x 13 mm.

2.3 Gamma detector

Six gamma detectors based on BGO crystals with a diameter of 76 mm and thickness of 65 mm were used to detect gamma quanta from the irradiated object.

These detectors have the following features:

(1) Satisfactory energy resolution (8–2.5 %) within the energy range of 1 to12 MeV. for the carbon gamma line (E_γ = 4.43 MeV) The energy resolution of the gamma detector is on average Γ_E = (4.4 ± 0.1)%.

(2) High efficiency of gamma detection within the specified energy range.

(3) Low sensitivity for detection of background neutrons.

The time resolution of the (α-γ)-coincidence system averaged over the whole set of the gamma detectors is Γ_t = (3.1±0.1) ns.

2.4 Data collection system

The recording electronics of the data acquisition system for the alpha and gamma detectors is designed as a single board with 32 inputs, which has the size of a standard PCI card and can be inserted in a PCI-E slot of a personal computer (PC). Information exchange with the PC is via the PCI-E bus. The data acquisition system is based on signal digitization with subsequent restoration of

the time and amplitude characteristics of the pulses from the alpha and gamma detectors. In order to ensure the required rate of data transmission via the PCI bus the board operates in the direct memory access mode.

The data acquisition system also includes the appropriate software consisting of a basic module (driver), control program, and reconstruction program. The data collection board performs direct digital conversion of signal pulses coming from the alpha and gamma detectors. It has built-in trigger circuits for operation in three (time, energy single-channel, alpha–gamma coincidence) modes. The software allows the amplitude and time characteristics of the signal to be accurately restored. The software operates under the Linux operating system.

3. Examined samples

For this investigation ALROSA supplied us with diamond simulants and waste kimberlite and core samples from wells. At the first stage we received 5 diamond simulants made of diamond powder, 6 kimberlite samples, and 3 core samples. The diamond simulants ranged in weight from 0.3 to 11.2 g and in overall dimensions from 5 to 20 mm, respectively. The linear dimensions of the kimberlite stones were around 8-15 cm with corresponding widths of 2-4 cm. The core samples were cylinders 10 cm in diameter and 20 cm in length.

At the second stage of the investigation we were provided with 55 kg of kimberlite from the "Mir" mining storehouse.

The kimberlite samples that we received at the second stage were rocks of irregular shape with typical linear dimensions 10–20 cm and thickness 4–10 cm.

4. Measurement procedure

Since diamonds entirely consist of carbon, the procedure of their detection consists in detecting excess carbon in any area of the kimberlite sample. The energy spectrum of characteristic carbon emission in reaction (2) is given in Fig. 3.

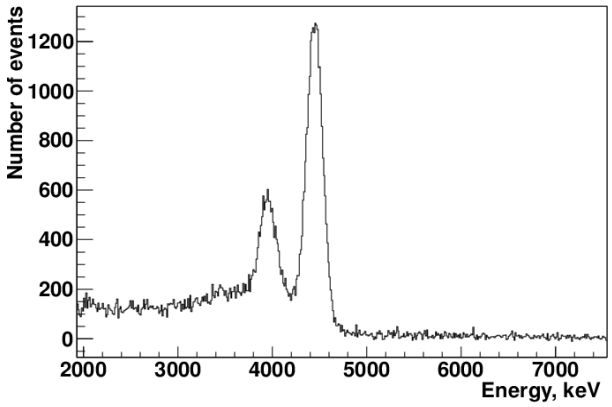

Fig. 3. Energy spectrum of gamma quanta for graphite (carbon).

As Fig. 3 shows, the 4.44-MeV gamma line uniquely points to the presence of carbon (diamond). Moreover, a single escape peak corresponding to an energy of 3.93 MeV is clearly observed. This simple shape of the carbon gamma spectrum significantly simplifies carbon detection in kimberlite.

The energy spectrum of the gamma quanta from the kimberlite is shown in Fig. 4 (blue line). Oxygen lines at 6.13 MeV and 3.8 MeV are clearly observed. At the same time there is no carbon peak at 4.44 MeV. This also simplifies diamond identification.

To simulate the spectrum of diamond-bearing kimberlite, we attached a graphite cube of 25 mm to the kimberlite sample. The spectrum from this assembly is shown in Fig. 4 (solid line).

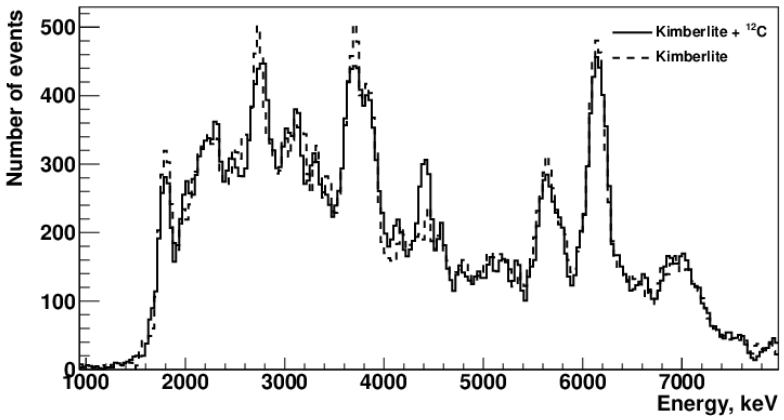

Fig. 4. Energy spectrum of gamma quanta from a kimberlite sample (solid line) and from a kimberlite + graphite cube assembly (dashed line).

One can clearly see that presence of carbon results in a peak at 4.44 MeV, which is absent in pure kimberlite (Fig. 4, dashed line).

A typical diamond simulant test is irradiation of the kimberlite + simulant assembly (see Fig. 2). The assembly is placed at a distance of 14 cm from the neutron generator, and the distance from the assembly to the gamma detectors is 30 cm. The neutron generator intensity is $I = 5 \times 10^7$ s^{-1}. The standard data-taking time is 30 min. We would like to emphasize that this time was chosen only for obtaining larger statistics to check the diamond detection procedure.

The sample irradiated with tagged neutrons is divided into 64 cells, and the elemental composition is determined in each cell. For further analysis only events within the range of 4.2–4.6 MeV corresponding to the carbon line are chosen. In each cell i, a value $\Delta_i = N\text{-}N_i$ was calculated, where N is the average number of events in the area of the carbon peak for the whole specimen and N_i is the number of events in the carbon peak region for this cell.

5. Measurement results

Figure 5 shows the distribution of the values $\Delta_i = N\text{-}N_i$ for a kimberlite sample.

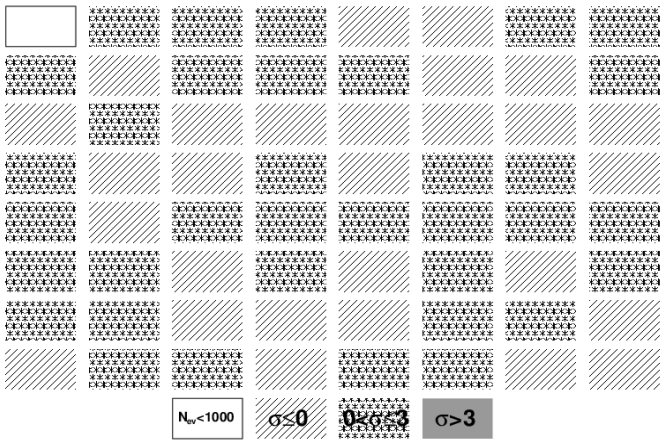

Fig. 5. Distribution of $\Delta_i = N-N_i$ for a kimberlite sample. Cells with $\Delta_i < 3\sigma$, where σ is the statistical error, are filled with stars, cells with $\Delta_i > 3\sigma$ are shown in grey. The regions with poor statistics are shown by empty rectangles. The cells with negative Δ_i are hatched.

One can see that deviations from the average are no larger than 3σ over the whole area of the sample. This is what is precisely expected for a homogeneous sample, where deviations of the carbon content from the average value are only due to statistical fluctuations.

Six kimberlite samples and three core samples exhibit no large Δ_i fluctuations, which is notable since the energy spectra of core samples indicate a clear signal from carbon fraction as shown in Figure 6.

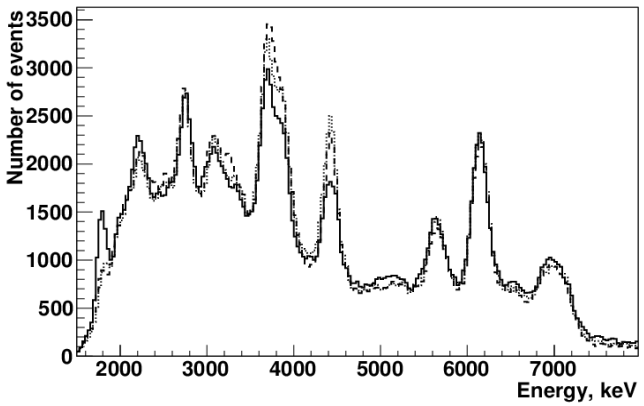

Fig. 6. Energy spectrum of gamma quanta of 3 core samples (shown in different line styles).

Figure 6 distinctively shows the carbon peak at 4.44 MeV. However, carbon presence in the elemental composition of the core sample did not result in a change in the *local* carbon concentration.

Figure 7 shows the results of processing the data on irradiation of an assembly of a 2-mm-thick kimberlite stone and an 11.2-g diamond simulant. The simulant is placed at the centre of the examination area within the range of the cell marked in grey in Fig. 7. The size of the simulant is 20 mm, while the size of one tagged beam at this distance is 11 mm. Thus, the carbon excess signal should be seen in several cells.

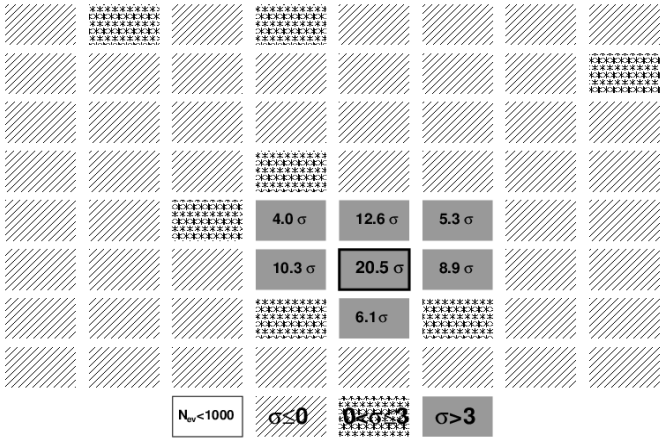

Fig. 7. Distribution $\Delta_i = N-N_i$ for irradiation of kimberlite assembly No. 1 (thickness 2 cm) and diamond simulant No. 6 (weight 11.2 g). Cells with $\Delta_i < 3\sigma$, where σ is the statistical error, are filled with stars, cells with $\Delta_i > 3\sigma$ are shown in grey. The regions with poor statistics are shown be empty rectangles. The cells with negative Δ_i are hatched.

Indeed, in group of several central cells excess above the statistical fluctuation limit by 3 σ is clearly observed. The excess of the recorded number of events in the carbon line above the average number of events for the sample is 20.5σ. Thus, the signal is very distinct and definitely associated with the presence of the diamond simulant.

The irradiation of other kimberlite samples with the diamond simulants gives the similar pattern as in Fig.7. The position of the diamond simulant in the kimberlite stone is correctly reproduced. The minimal detectable mass of the diamond simulant is 1.15 g behind the kimberlite 1 cm thick.

Upon completion of the first operation stage ALROSA supplied us with 33 kimberlite samples with a total weight 55 kg (see Fig. 8). The samples had a typical linear size of 15–20 cm and a weight of 1–2 kg.

Fig. 8. Kimberlite samples received at the second stage.

When examining the kimberlite samples using the above mentioned procedure, we did not found any statistically significant excess of the local carbon content above the average value was in 32 out of

33 stones. The observed deviation from the average value in all samples was no larger than 2.5σ. This indicates that the proposed procedure is characterized by a small false positive alarm rate (although statistics for confirmation of this statement is not sufficient yet).

In one of the samples (No. 17) a significant local carbon content excess above the average is detected. It ranges from 3.3 to 5.8σ depending on the angle at which the sample is irradiated.

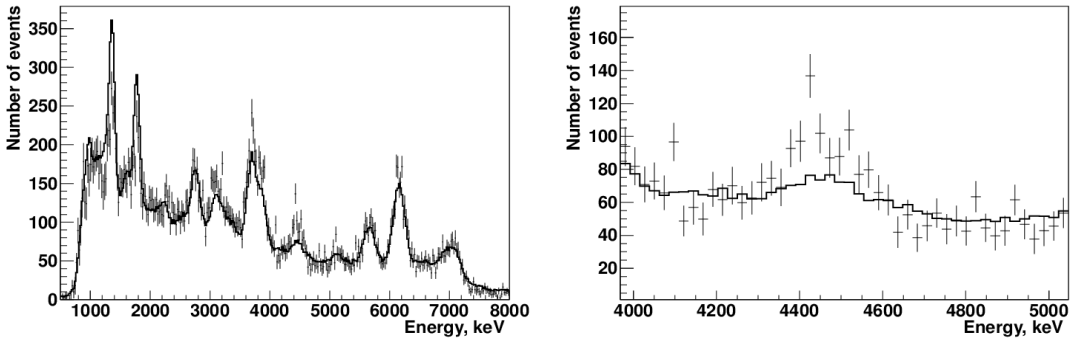

Fig. 9. Energy spectrum of gamma quanta from kimberlite sample No.17 (dots with error bars). The black solid line corresponds to the average spectrum of gamma quanta from the other kimberlite samples (left). The region of the spectrum around the carbon line is shown on the right plot.

After the samples were samples returned to ALROSA JSC, sample No. 17 with excess carbon was analyzed there. Two inhomogeneous diamond inclusions with diameter up to 7 mm consisting of small diamond crystals with size from 1 to 2 mm were discovered. The photo of the diamond inclusions is given in Fig. 10.

Fig. 10. Two diamond inclusions found in kimberlite sample No.17.

Thus, the ability of the tagged neutron method to detect diamonds in kimberlite was experimentally proved.

6. Conclusions

The technology for diamond detection in kimberlite based on the tagged neutron method is developed. An experimental setup based on a portable neutron generator with a built-in 64-pixel silicone alpha detector is created. The energy spectrum of the gamma quanta from kimberlite is measured by 6 BGO gamma detectors. Diamonds are identified by detecting a local carbon excess in the examined sample.

Measurements with 6 kimberlite and 3 core samples do not show any local excess of the number of events above the average in the carbon line region, whereas measurements with a combination of diamond simulants and kimberlite samples of different size and weight show the local excess of the number of events around 4.44 MeV. The minimal detectable mass of a diamond simulant is 1.15 g with a 1-cm-thick screening kimberlite layer in front of the simulant.

The subsequent check of the identification algorithm on 33 kimberlite samples with a total weight of 55 kg confirmed the potential of the tagged neutron method: false alarms were not detected, and the sample with a local carbon content excess from 3.3 to 5.8 σ was found to have two inhomogeneous diamond inclusions up to 7 mm in diameter consisting of small particles with a size of 1 to 2 mm.

Authors are grateful to the employees of the Dukhov All-Russian Research Institute of Automatics, particularly E. P. Bogolyubov, Yu. K. Presnyakov, V. I. Ryzhkov, T. O. Khasayev, A. S. Chuprikov, and D. I. Yurkov for creation of the neutron generator with unique parameters, and to the employees of ALROSA, particularly A. S. Chaadyev and O. E. Kovalchuk for very helpful comments.

References

1. **Yu. P. Solodova, M. V. Nikolayev, K.K. Kurbatov** et al., Diamond Gemmology, Moscow, 2008. – 416 pages.
2. **P. O. Hawkins, R. W. Sutton**, Rev. Sci. Instr. 31 (1960) 241.
3. **L. I. Ussery** et al., Los Alamos Nat. Lab report LA12847-MS (October 1994).

4. **E. Rhodes** et al., SPIE, v. 2092, p. 288 (1993); E. Rodes et al., IEEE Trans. Nucl. Science, 39 (1992) 1041–1045.
5. **A. Beyerle, J. P. Hurley, L. Tunnell**, Nucl.Instr.Meth. A299 (1990) 458.
6. **S. Pesenti** et al., Nucl. Instr. Meth., A531 (2004) 657.
7. **V. M. Bystritsky** et al., Proceedings of the 4th International Symposium on Technology and Mine Problem, Naval Postgraduate School, March 13-16, Monterey, California, 2000.
8. **V. M. Bystritsky** et al., Proceedings of the International Conference on Requirements and Technologies for the Detection, Removal and Neutralization of Landmines and UXO, EUDEM2-SCOT-2003, 15-18 September 2003, Vrije Universiteit Brussel, Brussels, Belguim, 2003, v 1,2.
9. **V. M. Bystritsky** et al., Proc. Conference "Portable neutron generators and technologies on their basis", Moscow, 2004, p. 283.
10. **V. M. Bystritsky** et al., JINR Communications, E13-2006-36, 2006.
11. **V. M. Bystritsky** et al., Physics of Particles and Nuclei Letters, 5 (2008) 441.
12. **V. M. Bystritsky** et al., Physics of Particles and Nuclei Letters, 5 (2013) 722.